Generation of picoliter and nanoliter drops on demand in a microfluidic chip

Jie Xu and Daniel Attinger

Laboratory for Microscale Transport Phenomena, Department of Mechanical Engineering,
Columbia University, New York, NY 10027, USA, da2203@columbia.edu

ABSTRACT

In this work, we introduce the novel technique of *in-chip drop on demand*, which consists in dispensing picoliter to nanoliter drops on demand directly in the liquid-filled channels of a polymer microfluidic chip, at frequencies up to 2.5 kHz and with precise volume control. The technique involves a PDMS chip with one or several microliter-size chambers driven by piezoelectric actuators. In this article, the drop formation process is characterized with respect to critical dispense parameters such as the shape and duration of the driving pulse, and the size of both the fluid chamber and the nozzle. Several features of the in-chip drop on demand technique with direct relevance to lab on a chip applications are presented and discussed, such as the precise control of the dispensed volume, the ability to merge drops of different reagents and the ability to move a drop from the shooting area to a contraction.

Keywords: microfluidics, drop on demand, ink-jet

1 INTRODUCTION

The concept of lab on a chip, where a tiny fluid microprocessor performs complex analysis and synthesis tasks relevant to chemistry or biology has drawn great interest since the early 1990's [1, 2]. Several achievements have demonstrated that shrinking a chemical or biological laboratory into a microchip could have significant benefits such as increased sensitivity, fast response time, low reagent and sample consumptions, as reviewed in [2-5]. The ability to dispense and control small liquid volumes in the microchannels is critical for the lab on a chip technology, and several techniques address this issue. For instance, pinching by electrokinetic process [6] or the volumetric change induced by a piezoelectric actuator [7] have been used to inject individual liquid plugs in a miscible liquid. Also the segmented flow technique has been developed: it uses syringe pumps feeding two branches of a T-connection [8-10] or two concentric channels [11, 12] and forms a train of drops inside microchannels. The segmented flow has the advantage over the electrokinetic pinching that the diffusion between the minute amount of liquid dispensed and the carrying fluid is minimal. Both methods are suited for performing complex, multistep analysis or synthesis [13, 14]. However, the ability to dispense and manipulate a single particle rather than a train of particles would be welcome in order to handle expensive reagents or analyze individual biological cells. Indeed, George Whitesides, the Harvard professor who fathered soft microfluidics, mentioned this need in 2007. Cited in Nature Methods [15] he describes the use of bubbles in microfluidic chips, and concludes: "There is a particular bit of the puzzle that needs to be added, which will not be hard to do but it has not been done yet—that is, bubble on demand". While the well-established ink-jet technology dispenses individual drops, on demand, *into the atmosphere* [16], few processes are able to generate particles on demand *into a microfluidic chip*: individual drops can be generated using voltages of 1kV producing a Taylor cone at a water-oil interface with subsequent breakup [17]; also, the back-and-forth motion of an interface can be carefully controlled with a syringe pump to generate a single drop [18]; further, a single bubble has been generated by thermally expanding gas in a chamber until the protruding meniscus is broken into a bubble by a shear flow [19]. While successful at generating a single particle, these techniques rely on complex external actuation and the accuracy of the timing and generated volume was either low [17, 18] or not quantified [19]. In this paper, we present a technique to precisely dispense a single drop on demand in a microfluidic chip with a local piezoelectric actuator.

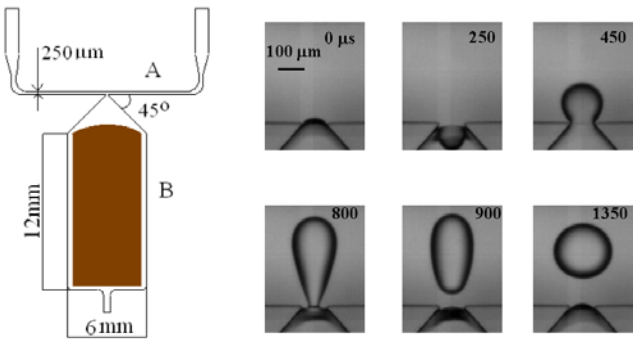

Figure 1: (a) A typical chip geometry consisting of oil-filled channel *A* and water-filled chamber *B*. A piezoelectric bimorph actuator is glued to the chamber *B* allows the release of an aqueous drop on demand in the channel A. (b) Stages depicting of the formation of a 1nL drop from a 50 µm nozzle.

2 DESIGN, FABRICATION AND SETUP

The typical design of a microfluidic chip used in our study is shown in Figure 1a: it involves one or several µL-volume reagent chambers such as *B* connected via a 25-100 µm nozzle to a main channel *A*. The main channel is filled

with hexadecane while each chamber *B* can be filled with water. Since the water-hexadecane system is immiscible, a stable meniscus forms at the nozzle opening. The height of the channels is in the 50-100 μm range. The chip is sealed with a thin membrane. A piezoelectric actuator is placed on top of each chamber, to modify the chamber volume and release an aqueous drop, on demand, in the main channel. This drop generation process is shown in Figure 1b. Drop volumes as small as a few pL and the internal flow associated with the motion of drops in a channel [7] enhance mixing and diffusion.

Microfluidic chips were fabricated using soft lithography [20]. First, a 50-100 μm layer of *SU-8* is cured on top of a wafer with patterns transferred from a transparency mask. The chip is then manufactured from the master using PDMS Sylgard 184 Kit (Dow Corning). The channels are sealed by a thin 180 μm membrane made from spin-coated PDMS. The piezoelectric actuators are commercially available bimorph actuators made of two PZT layers bonded on a thin brass layer, with a total thickness *T* of 0.51 mm, with lengths and widths slightly smaller than the chamber dimensions as shown in Figure 1a and as given in Table 1. One actuator is then taped on top of each chamber, using a 90 μm layer of double-sided tape.

The experimental setup involves the microfluidic chip described above and a 20MHz function generator (Agilent, 33120A) coupled to a 1MHz 40W amplifier (Krohn-Hite, 7600M), which generates high-voltage driving pulses for the actuators glued on the microfluidic chip. We use Olympus IX-71 microscope and a high-speed camera (Redlake MotionXtra HG-100K) as sensing system.

Symbol	Physical property	Typical Value
γ	Surface tension at the water-hexadecane interface	52.5 mJ/m^2 [21]
d_{31}	Piezoelectric strain coefficient	190×10^{-12} Pa
Y	Piezoelectric elastic modulus	6.2×10^{10} Pa
ρ	PZT density	7750 kg/ m^3
E	Electric field applied across actuator	400 kV/m
L, B, T	Actuator length, width, thickness	12-20, 3-4, 0.51 mm

Table 1: Physical properties and typical values

3 ANALYSIS AND CHARACTERIZATION

3.1 Motion of the Actuator

An important parameter in the actuation design is the eigenfrequency of the actuator, which limits the speed of deformation. The eigenfrequency f_n of a piezoelectric bimorph with $L>>w$ is given in [22] for two types of boundary conditions: anchored at one end as $f_n = (0.16T/L^2)\sqrt{Y_{11}/\rho}$, or anchored at one end and with the other end immobile along the z-direction, as $f_n = (0.48T/L^2)\sqrt{Y_{11}/\rho}$. While none of the boundary conditions is exactly the experimental conditions, the latter was found in better agreement to our measurements.

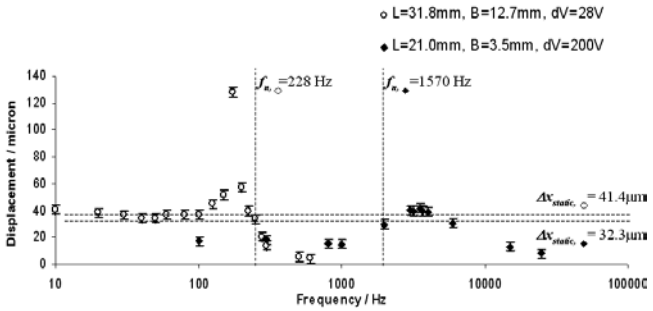

Figure 2: Influence of the excitation frequency on the amplitude of the actuator motion. The empty circles and full lozenges denote two types of boundary conditions. The dashed lines denote the theoretical values for natural frequency and static displacement.

Using an Optem long distance microscope objective and a high-speed camera, we measured the temporal deformation of an actuator driven by a single rectangular pulse of amplitude *dV* and duration $(2f)^{-1}$. Figure 2 summarizes these measurements, showing the maximum observed displacement as a function of the frequency *f* of the driving pulse. A first series of measurements, shown by empty circles, is made for a relatively large bimorph clamped at one end, with dimensions given in Figure 2. Theoretical values are also plotted as dashed lines for both the maximum static displacement and the eigenfrequency. The agreement is relatively good in terms of resonance frequency and static (low frequency) displacement. The lower resonance frequency observed experimentally can be explained by the difficulty to experimentally anchor one end of the actuator in a perfect way because we used a C-clamp. A second series of measurements is made with a smaller actuator attached via double-sided tape to a 180 μm thin PDMS layer. The two ends of the PDMS layer are then anchored firmly between two C-clamps, each clamp being about 1.5 mm away from the corresponding end of the piezo. While both the actuator size and configuration are close to the design of the microfluidic chip, the configuration is close but not exactly corresponding to the second type of boundary condition presented above: this might explain why the measured static displacement and resonance frequencies are different, both being larger than the theoretical values. Importantly, the visualization shows that the actuator does not freeze its motion once the driving pulse vanishes, but keeps oscillating at its natural frequency for about 6 periods. This behavior due to the relatively large size and inertia of the actuator, and the very soft, thin PDMS sealing layer contrasts with existing piezoelectric drop on demand dispensers and the relative modelings [23-26],

where the chamber walls are much stiffer, typically made of glass [23] or silicon [27].

3.2 Effects of Driving Pulse on the Drop Formation

Characterization experiments reported in Figure 3 describe how the drop volume is influenced by the nozzle size, the pulse shape and the pulse duration. All the data in Figure 3 was obtained with an actuation voltage of +/- 200V. The chamber lengths used for the respective 50 and 100 μm nozzle case were 12mm and 20mm, respectively. The shape of the pulse corresponds to an initial expansion of the chamber for a time t_1 followed by compression for a time t_2. Pulses with $t_1=0$ were also successful at generating a drop: they correspond to simple compression of the chamber. Figure 3 shows that drops with volumes from 25 pL to 4.5 nL can be generated by varying the pulse shape and the nozzle size. For a given nozzle geometry, the drop volume can be controlled by the pulse shape within one order of magnitude. Pulses with durations too different from an optimum duration will not produce any drop. For the 50 μm nozzle we also observe some dual-dispense states where two smaller drops are simultaneously produced, by the *Mickey Mouse instability* process described in section 4 and shown in Figure 4d. Also, in Figure 3, crosses demonstrate how the drop volume can be controlled by changing the ratio between the expansion time and the compression time, while keeping the total actuation time constant.

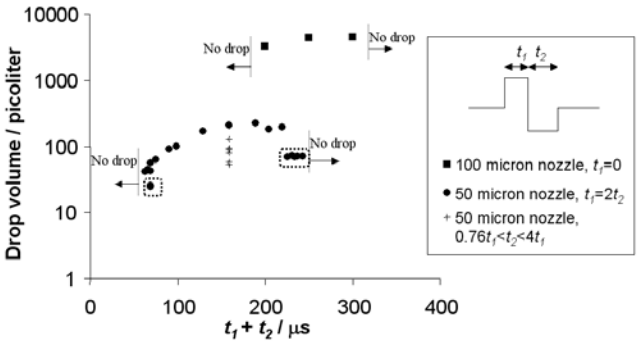

Figure 3: Drop volumes as a function of dispense parameters. The horizontal axis denotes the total pulse length, which involves the chamber expansion followed by the chamber compression, with respective duration t_1 and t_2. The channel height is the same as the nozzle width. The dotted rectangles show *Mickey Mouse* dispenses.

The results in Figure 2 and Figure 3 suggest that the optimum pulse duration to produce drops corresponds to the natural frequency f_n of the actuator. Indeed, the second equation presented in section 3.1 predicts values of f_n of 1.57 kHz, respectively 4.74 kHz for the actuators of the chambers with respectively the 100 μm and 50 μm nozzle. The corresponding single pulse duration for the 100 μm nozzle would be $t_2=1/(2\,f_n)$=318 μs, a time close to the 180-300 μs interval effective at producing drops in Figure 3. Similarly, the corresponding total pulse duration for the 50 μm nozzle, in the case of a pulse with $t_1=t_2$, would be $t_1+t_2=1/f_n=211\ \mu s$, a time close to the 60-220 μs interval effective at producing drops in Figure 3. The fact that the pulse duration estimated theoretically is at the higher end of the interval of experimentally successful durations might simply indicate that the actual value of f_n is slightly higher than the theoretical value, a fact shown in Figure 2.

We also tried to quantify the maximum dispense rate by repeating the driving pulse with smaller and smaller time interval between pulses. Experiment shows that drops are still generated even if the time interval is reduced to 0s, which corresponds to applying the generation pulse continuously. For example, in a case where a 400 μs pulse, shaped as in Figure 3 with $t_2 = 2t_1$, is applied continuously to the piezoactuator and a train of drops were successfully generated at 2.5 kHz. In addition, we studied the uniformity of the drop volumes. At a dispense rate of 6.2 Hz, 20 drops generated had an average volume of 1023 pL and a standard deviation of 16 pL, which corresponds to less than 2%.

4 FEATURES RELATED TO LAB ON A CHIP

The in-chip drop on demand technique has the potential to perform in-chip reagent mixing, transport and multistep reactions. Three features of the *in-chip drop on demand* technique with direct relevance to lab on a chip applications are presented in Figure 4.

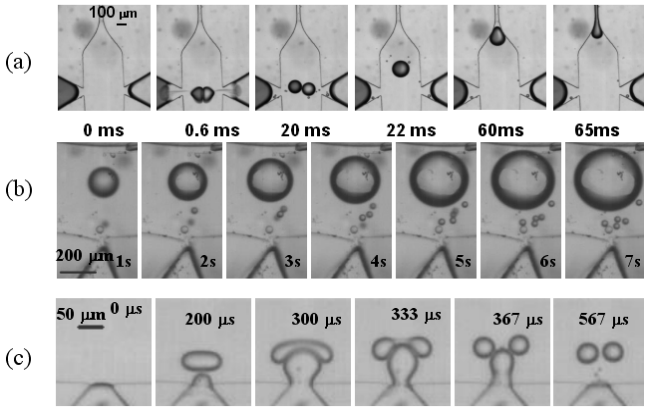

Figure 4: Three features of in-chip drop on demand with relevance to lab on a chip applications: (a) merging and mixing of two different reagents and transport to a contraction (b) digital control of drop volume, and (c) *Mickey Mouse* dispense, where two drops of small volume are generated simultaneously by a single pulse.

Figure 4a shows the ability of mixing different reagents into a single drop. The nozzle on the left generates a drop of ink while the right nozzle generates a pure water drop. Coalescence occurs and then the drop is transported into a contraction which can enhance the mixing inside the drop. This feature enables precise-controlled reactions in drops.

Figure 4b shows the second feature, which is the ability to digitally control the dispensed drop volume, by generating additional drops that coalesce with the original drop. The first frame shows a 500 pL drop whose volume is increased to 3.5 nL by 6 successive increments of 500 pL. This coarse, digital way to control the drop volume can be coupled with the finer, analog volume control by modifying

the pulse parameters in order to exactly dispense the desired quantities over a wide range of volumes.

Figure 4c show the third feature, which is the ability to generate a dual-state drops, while applying a single excitation pulse to the actuator. This occurs when an initially generated drop is hit by a strong subsequent excursion of the meniscus. During the process, the meniscus breaks the initial drop into two half drops while briefly assuming the shape of Mickey Mouse, the well-known cartoon character (367 μs). Therefore, we call this type of dispense the *Mickey Mouse* dispense.

5 CONCLUSION AND OUTLOOK

The *in-chip drop on demand* technique presented in this article allows the individual generation of drops of aqueous reagents in a microfluidic chip with a temporal precision of one millisecond, and at rates higher than one kHz. The ability to precisely trigger the drop generation time will allow the coordination of the generation of drops with events occurring in the chip, such as the detection of chemical reaction or temperature changes, or the transit of biological cells and other particles. The drop volume can be controlled from 40 pL to 4.5 nL by varying the pulse shape, the chip geometry, or by merging several drops together.

Acknowledgements:

This work has been supported partially by NSF grants 0449269 and 0701729.

REFERENCES

1. Manz, A., et al., Advances in Chromatography, 1993. **33**: p. 1-66.
2. Lion, N., et al., Electrophoresis, 2003. **24**(21): p. 3533-3562.
3. Verpoorte, E. and N.F. De Rooij, Proceedings of the Ieee, 2003. **91**(6): p. 930-953.
4. Stone, H.A., A.D. Stroock, and A. Ajdari, Annual Review of Fluid Mechanics, 2004. **36**: p. 381-411.
5. Whitesides, G.M., Nature, 2006. **442**(7101): p. 368-373.
6. Bai, X., et al., Lab Chip, 2002(2): p. 45-49.
7. Guenther, A., et al., Lab Chip, 2004. **4**: p. 278-286.
8. Song, H., D.L. Chen, and R.F. Ismagilov, Angewandte Chemie-International Edition, 2006. **45**(44): p. 7336-7356.
9. Gunther, A., et al., Langmuir, 2005. **21**(4): p. 1547-1555.
10. Thorsen, T., et al., Physical Review Letters, 2001. **86**(18): p. 4163-4166.
11. Jensen, M.J., H.A. Stone, and H. Bruus, Physics of Fluids, 2006. **18**(7).
12. Anna, S., N. Bontoux, and H. Stone, App. Phys. Lett., 2003. **82**(3): p. 364.
13. Fair, R., Microfluid Nanofluid, 2007. **3**(245-281).
14. Ismagilov, R.F., et al., Faseb Journal, 2007. **21**(5): p. A42-A42.
15. Blow, N., Nature Methods, 2007. **4**: p. 665-668.
16. Le, H., JOURNAL OF IMAGING SCIENCE AND TECHNOLOGY, 1998. **42**(1): p. 46-92.
17. He, M., J. Kuo, and D. Chiu, App. Phys. Lett., 2005. **87**: p. 031916.
18. He, M., et al., Anal. Chem., 2005. **77**: p. 1539-1544.
19. Prakash, M. and N. Gershenfeld, Science, 2007. **315**: p. 832-835.
20. Xia, Y.N. and G.M. Whitesides, Annual Review of Materials Science, 1998. **28**: p. 153-184.
21. Lee, S., D. Kim, and D. Needham, Langmuir, 2001. **17**: p. 5537–5543.
22. Smits, J. and W. Choi, IEEE Transactions Ultrasonics Ferroelectrics Frequency Control, 1991(38): p. 256-270.
23. Dijksman, J.F., Journal of Fluid Mechanics, 1984. **139**: p. 173-191.
24. Bogy, D.B. and F.E. Talke, ibm journal research and development, 1984. **28**(3): p. 314-321.
25. Hayes, D.J., D.B. Wallace, and M.T. Boldman. *ISHM Symposium 92 Proceedings*. 1992.
26. Wallace, D.B., ASME publication 89-WA/FE-4, 1989.
27. Nguyen, N. and S. Wereley, *Fundamentals of Microfluidics*. 2002: Artech House.